Purification and Characterization of Novel Microtubule-Associated Proteins from Arabidopsis Cell Suspension Cultures[1][C][W]

Takahiro Hamada[2,3], Nahoko Nagasaki-Takeuchi[2], Takehide Kato, Masayuki Fujiwara, Seiji Sonobe, Yoichiro Fukao, and Takashi Hashimoto*

Graduate School of Biological Sciences (T.Ham., N.N.-T., T.K., T.Has.) and Plant Global Education Project, Graduate School of Biological Sciences (M.F., Y.F.), Nara Institute of Science and Technology, Ikoma, Nara 630–0192, Japan; and Graduate School of Life Science, University of Hyogo, Kamigori-cho, Ako-gun, Hyogo 678–1297, Japan (S.S.)

Plant microtubules (MTs) play essential roles in cell division, anisotropic cell expansion, and overall organ morphology. Microtubule-associated proteins (MAPs) bind to MTs and regulate their dynamics, stability, and organization. Identifying the full set of MAPs in plants would greatly enhance our understanding of how diverse MT arrays are formed and function; however, few proteomics studies have characterized plant MAPs. Using liquid chromatography-tandem mass spectrometry, we identified hundreds of proteins from MAP-enriched preparations derived from cell suspension cultures of Arabidopsis (*Arabidopsis thaliana*). Previously reported MAPs, MT regulators, kinesins, dynamins, peroxisome-resident enzymes, and proteins implicated in replication, transcription, and translation were highly enriched. Dozens of proteins of unknown function were identified, among which 12 were tagged with green fluorescent protein (GFP) and examined for their ability to colocalize with MTs when transiently expressed in plant cells. Six proteins did indeed colocalize with cortical MTs in planta. We further characterized one of these MAPs, designated as BASIC PROLINE-RICH PROTEIN1 (BPP1), which belongs to a seven-member family in Arabidopsis. BPP1-GFP decorated interphase and mitotic MT arrays in transgenic Arabidopsis plants. A highly basic, conserved region was responsible for the in vivo MT association. Overexpression of BPP1-GFP stabilized MTs, caused right-handed helical growth in rapidly elongating tissues, promoted the formation of transverse MT arrays, and resulted in the outgrowth of epidermal cells in light-grown hypocotyls. Our high-quality proteome database of Arabidopsis MAP-enriched preparations is a useful resource for identifying novel MT regulators and evaluating potential MT associations of proteins known to have other cellular functions.

Microtubules (MTs) are major structural components of the plant cytoskeleton that are composed of α-tubulin/β-tubulin heterodimer subunits and are intricately involved in cell division, morphology, and intracellular organization and transport. The ability of the MT cytoskeleton to fulfill its versatile cellular functions relies on its intrinsically dynamic polymer properties. Individual MTs alternate between phases of growth and shrinkage by rapidly attaching and removing tubulin subunits at their ends. These cycles of polymerization and depolymerization, which continuously reorganize the MT cytoskeleton, are sometimes interrupted by pauses in which neither growth nor shrinkage occurs (Desai and Mitchison, 1997). Numerous proteins regulate the dynamic equilibrium between tubulin subunits and assembled MTs and facilitate interactions between two neighboring MTs and between MTs and other cellular components (Mandelkow and Mandelkow, 1995; Maiato et al., 2004). These MT regulators organize diverse MT arrays, transporting organelles to subcellular compartments and scaffolding the proteins that function in signal transduction events. In this paper, we define such MT regulators as microtubule-associated proteins (MAPs), although this terminology classically referred to proteins that copurify with MTs from cell extracts (Lloyd and Hussey, 2001).

To date, several dozen plant MT regulators have been identified using three distinct strategies (Hamada, 2007; Sedbrook and Kaloriti, 2008). First, since some MAPs exhibit conserved amino acid sequences, plant homologs of animal and fungal MAPs have been identified by bioinformatic searches (Gardiner and Marc, 2003). Second, genetic screens for Arabidopsis (*Arabidopsis*

[1] This work was supported by Grants-in-Aid from the Ministry of Education, Culture, Sports, Science, and Technology of Japan (grant nos. 23012028 and 24114004 to T.Has.) and from the Japan Society for the Promotion of Science (grant no. 23247008 to T.Has. and research fellowship no. 11J01084 to T.Ham.).

[2] These authors contributed equally to the article.

[3] Present address: Department of Life Sciences, Graduate School of Arts and Sciences, University of Tokyo, Komaba, Tokyo 153–8902, Japan.

* Address correspondence to hasimoto@bs.naist.jp.

The author responsible for distribution of materials integral to the findings presented in this article in accordance with the policy described in the Instructions for Authors (www.plantphysiol.org) is: Takashi Hashimoto (hasimoto@bs.naist.jp).

[C] Some figures in this article are displayed in color online but in black and white in the print edition.

[W] The online version of this article contains Web-only data.

www.plantphysiol.org/cgi/doi/10.1104/pp.113.225607

thaliana) mutants altered in anisotropic growth or sensitivity to MT-interacting drugs have revealed various proteins required for MT organization and stability, some of which are only present in plants (Ishida et al., 2007a). Third, MAPs were purified from crude plant cell extracts, based on their ability to bind MTs. MTs in cell extracts polymerize in the presence of the MT stabilizer taxol and depolymerize upon drug washout under MT-destabilizing conditions, such as high concentrations of salt and calcium and low temperature. Repeated polymerization/depolymerization cycles highly enrich for cytoplasmic proteins that bind MTs directly or indirectly.

It is often challenging to purify tubulins and copurify MAPs in sufficient quantity and quality from plant sources, largely due to the presence of the cell wall and large central vacuoles. Evacuolated, cytoplasm-rich miniprotoplasts prepared from cultured tobacco (*Nicotiana tabacum*) cells contain sufficiently high concentrations of endogenous tubulins for taxol-induced polymerization and have been successfully used to isolate major tobacco MAPs, such as MAP65 (Chang-Jie and Sonobe, 1993), MAP190 (Igarashi et al., 2000), and MAP200, a tobacco homolog of Arabidopsis MICROTUBULE ORGANIZATION1 (MOR1; Hamada et al., 2004). Fifty-five proteins, including kinesins, MAP65 isoforms, MOR1, and MAP70, were identified from a MAP-enriched preparation made from Arabidopsis protoplasts and analyzed by liquid chromatography (LC)-tandem mass spectrometry (MS/MS; Korolev et al., 2005).

In this study, we purified MAP-containing fractions from evacuolated miniprotoplasts derived from Arabidopsis cell suspension cultures. We identified 727 proteins, including dozens of previously uncharacterized proteins and numerous established Arabidopsis kinesins and MAPs, using LC-MS/MS. Subsequent subcellular localization assays identified six of these proteins as

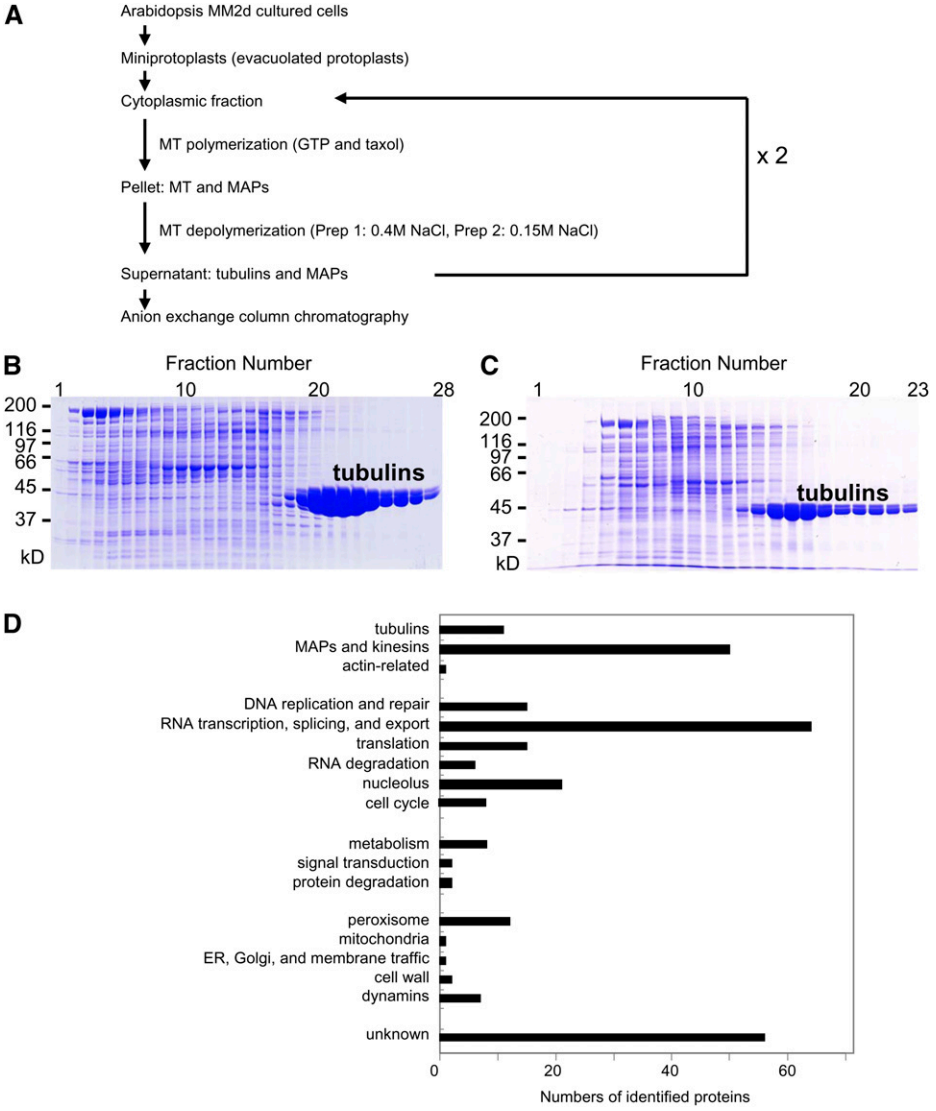

Figure 1. Purification of tubulins and MAPs from cultured Arabidopsis cells. A, Summary of the purification procedure. For details, see "Materials and Methods." B and C, Purified preparations analyzed by SDS-PAGE and stained with Coomassie Brilliant Blue. Representative fraction numbers after anion-exchange column chromatography are given above the gels. Tubulins are indicated. MT depolymerization steps were carried out in the presence of 0.4 M NaCl (B; preparation 1) or 0.15 M NaCl (C; preparation 2). D, Classification of 298 highly enriched proteins according to the Gene Ontology annotations. ER, Endoplasmic reticulum. [See online article for color version of this figure.]

Table I. *Identification of known MAPs*

The emPAI scores of known MAPs are shown. Asterisks indicate the proteins reported in the MAP preparation by Korolev et al. (2005).

Name	Arabidopsis Genome Initiative Code	emPAI Scores			Korolev et al. (2005)
		Preparation 1	Preparation 2	Crude	
MOR1	AT2G35630	5.35	14.08	0.05	*
CLASP (CLIP-ASSOCIATED PROTEIN)	AT2G20190	3.19	2.26	0	
EB1a (END-BINDING PROTEIN1a)	AT3G47690	0	0	0	
EB1b	AT5G62500	0	0	0	
EB1c	AT5G67270	0	3.31	0	
MAP65-1	AT5G55230	53.36	36.06	0.06	*
MAP65-2	AT4G26760	10.34	4.53	0	*
MAP65-3/PLEIADE	AT5G51600	1.24	0	0	
MAP65-4	AT3G60840	0.8	0	0	
MAP65-5	AT2G38720	4.25	2.61	0	
MAP65-6	AT2G01910	3.75	0	0	
MAP65-7	AT1G14690	2.14	0.05	0	
MAP65-8	AT1G27920	0	0	0	
MAP65-9	AT5G62250	0	0	0	
SPR2/TOR1 (SPIRAL2/tortifolia1)	AT4G27060	7.84	0.12	0	
SP2L (SPIRAL2-like)	AT1G50890	0.27	0	0	
SPR2-like (less related)	AT1G27210	0.53	0	0	
SPR2-like (less related)	AT5G62580	0.11	0	0	
SPR2-like (less related)	AT1G59850	0	0	0	
SPR2-like (less related)	AT2G07170	0	0	0	
MAP70-1	AT1G68060	0.87	33.65	0	*
MAP70-2	AT1G24764	0.59	10.24	0	
MAP70-3	AT2G01750	1.54	2.13	0	
MAP70-4	AT1G14840	0	1.92	0	
MAP70-5	AT4G17220	0	0	0	
WVD2 (WAVE-DAMPENED2)	AT5G28646	0	0	0	
WDL1 (WVD2-LIKE1)	AT3G04630	0	2.4	0	
WDL2	AT1G54460	1.85	6.38	0	
WDL3	AT3G23090	0.33	0.21	0	
WDL4	AT2G35880	0.59	16.36	0	
WDL5	AT4G32330	0.08	16.66	0	
WDL6	AT2G25480	0	1.63	0	
WDL7	AT1G70950	0	0	0	
Katanin p60 subunit	AT1G80350	0	1.91	0	
Katanin p80 subunit	AT1G61210	0	0.85	0	
Katanin p80 subunit candidate	AT5G08390	0	0.48	0	
Katanin p80 subunit candidate	AT1G11160	0	0	0	
Katanin p80 subunit candidate	AT5G23430	0	0	0	
TUBG1 (γ-tubulin)	AT3G61650	4.02	1.74	0	*
TUBG2 (γ-tubulin)	AT5G05620	2.84	0	0	*
GCP2 (γ-TUBULIN-CONTAINING COMPLEX PROTEIN2)	AT5G17410	0.92	0.52	0	
GCP3	AT5G06680	1.7	0.41	0	*
GCP4	AT3G53760	0.23	0	0	
GCP5a	AT1G80260	0.03	0	0	
GCP5b	AT1G20570	0	0	0	
GCP6	AT3G43610	0.05	0	0	
NEDD1	AT5G05970	0.09	0.19	0	
GIP1a (GCP3-INTERACTING PROTEIN1a; MOZART1a)	AT4G09550	0	0	0	
GIP1b (GCP3-INTERACTING PROTEIN1b; MOZART1b)	AT1G73790	0	0	0	
MPB2C (MOVEMENT PROTEIN BINDING2C)	AT5G08120	2.84	1.61	0	
AIR9 (AUXIN-INDUCED IN ROOT CULTURES9)	AT2G34680	1.63	1.44	0	
TPX2c (TARGETING PROTEIN FOR Xenopus Kinesin-like Protein2)	AT1G03780	0	0	0	
RUNKEL/EMB3013 (EMBRYO-DEFECTIVE3013)	AT5G18700	0.81	0.6	0	
MAP190/EMB1579 (EMBRYO-DEFECTIVE1579)	AT2G03150	1.75	2.58	0	
EDE1 (ENDOSPERM-DEFECTIVE1)	AT2G44190	0	0.15	0	
RIP2 (ROP INTERACTIVE PARTNER2)	AT2G37080	0	0	0	
MIDD1/RIP3	AT3G53350	0	0.48	0	
RIP5	AT5G60210	0	0.19	0	
RIP1 (MIDD1 less related)	AT1G17140	0	0	0	
RIP4 (MIDD1 less related)	AT1G78430	0	0	0	

Table II. *Identification of kinesins*

The emPAI scores of kinesins are shown. Asterisks indicate the proteins reported in the MAP preparation by Korolev et al. (2005).

Kinesin Family	Subgroup	Arabidopsis Genome Initiative Code	emPAI Scores			Korolev et al. (2005)
			Preparation 1	Preparation 2	Crude	
Plant-specific ungrouped		AT3G54870	0.73	0	0	
		AT1G01950	0.11	0.11	0	
		AT1G12430	0.07	0	0	
Family 1		AT3G63480	0	0	0	
Family 4		AT3G50240	0	0	0	
		AT5G47820	0	0	0	
		AT5G60930	0.82	0	0	
Family 5		AT2G28620	1.24	0.06	0	*
		AT3G45850	15.32	0.16	0	*
		AT2G37420	0.59	0	0	
		AT2G36200	1.84	0	0	*
Family 6		AT1G20060	0	0	0	
Family 7	NACK (NUCLEUS- and PHRAGMOPLAST-LOCALIZED PROTEIN KINASE1-ACTIVATING KINESIN) subgroup	AT1G18370	0	0	0	
		AT3G43210	0.07	0	0	
	Subgroup	AT2G21300	0	0	0	
		AT4G38950	0	0	0	
	Subgroup	AT3G51150	0	0	0	
		AT5G66310	0	0	0	
	Subgroup	AT4G24170	0	0	0	
		AT5G42490	0	0	0	
	MKRP (MITOCHONDRIAL KINESIN-RELATED PROTEIN) subgroup	AT1G21730	0.44	0	0	
		AT3G12020	3.08	0	0	
		AT5G06670	0	0	0	
		AT2G21380	0	0	0	
		AT4G39050	0.54	0	0	
	Subgroup	AT1G59540	0	0	0	
		AT3G10180	0	0	0	
Family 8		AT1G18550	0	0	0	
		AT3G49650	0	0	0	
Family 10	PAKRP2 (PHRAGMOPLAST-ASSOCIATED KINESIN RELATED PROTEIN2) subgroup	AT4G14330	0	0	0	
	Subgroup	AT5G02370	0	0	0	
		AT5G23910	0	0	0	
Family 12	Subgroup	AT3G17360	0	0	0	
		AT3G19050	0	0	0	
		AT3G44050	0	0	0	
	PAKRP1 subgroup	AT3G20150	0	0	0	
		AT3G23670	0	0	0	
		AT4G14150	0	0	0	
Family 13		AT3G16060	3.29	0	0	
		AT3G16630	1.65	0	0	
Family 14/Internal 1	ATK4 (ARABIDOPSIS THALIANA KINESIN4) subgroup	AT1G09170	0	0	0	
		AT5G27000	0	0	0	
		AT2G47500	0	0	0	
	Subgroup	AT1G18410	0	0	0	
		AT1G73860	0	0	0	
	Subgroup	AT1G63640	3.26	0.53	0	*
		AT5G41310	0	0	0	
	Subgroup	AT3G44730	0	0	0	
	Subgroup	AT3G10310	0	0	0	
Family 14/Internal 2		AT1G72250	0	0	0	
		AT2G22610	0.46	0	0	

(*Table continues on following page.*)

Table II. (*Continued from previous page.*)

Kinesin Family	Subgroup	Arabidopsis Genome Initiative Code	emPAI Scores			Korolev et al. (2005)
			Preparation 1	Preparation 2	Crude	
		AT5G27550	0	0	0	
Family 14/N-terminal 4		AT1G55550	0	0	0	
		AT5G27950	0	0	0	
Family 14/N-terminal 5		AT5G10470	0	0	0	
		AT5G65460	0	0	0	
Family 14/C-terminal 6		AT5G65930	0.13	0	0	
Family 14/C-terminal 8	Subgroup	AT4G05190	0.56	0.18	0	
		AT4G21270	0	0.38	0	*
	Subgroup	AT4G27180	13.11	0	0	*
		AT5G54670	8.44	0.14	0	

novel Arabidopsis MAPs. The Arabidopsis MAP proteome data set reported in this work will be valuable for future MT-related studies in the plant community.

RESULTS AND DISCUSSION

Purification of MAPs from Arabidopsis Cell Culture

We modified an existing MAP preparation protocol (Hamada et al., 2006, 2009), which was developed for tobacco BY-2 cell suspension cultures, to purify MAP-enriched protein fractions from Arabidopsis cell suspension cultures (Fig. 1A). Protoplasts were prepared from cultured Arabidopsis cells, and the vacuoles were removed by Percoll density gradient centrifugation. Soluble proteins extracted from the evacuolated miniprotoplasts were processed with two cycles of MT polymerization/depolymerization to enrich for proteins that have a high affinity for MT polymers. Two concentrations of NaCl (0.4 M in preparation 1 and 0.15 M in preparation 2) were used in the MT depolymerization buffers. Purified MAP-containing preparations were then separated by anion-exchange column chromatography, and proteins in major elution fractions were analyzed by LC-MS/MS. Highly acidic proteins, which were eluted from the column by high salt concentrations, were mostly composed of tubulins and were not analyzed further. SDS-PAGE and Coomassie Brilliant Blue protein staining revealed that the two MAP-enriched preparations contained tubulins as major proteins and had similar but distinct protein compositions (Fig. 1, B and C).

As a reference, we also subjected a crude protein preparation from the Arabidopsis miniprotoplasts to anion-exchange column chromatography and analyzed the eluted proteins by LC-MS/MS. SDS-PAGE analysis revealed that the protein composition of the reference preparation was distinct from that of the MAP-enriched preparations (data not shown).

Analysis and Assessment of MAP-Enriched Preparations by LC-MS/MS

Individual fractions or combined samples of three consecutive fractions (in the case of MAP preparation 1),

Table III. *Subcellular localization of GFP-fused MAP candidates*

Candidate MAP proteins were fused to GFP at their N or C terminus and expressed transiently in onion epidermal cells. The proteins are listed according to the order of the emPAI scores, with the highest scores in either preparation 1 or 2 at the top.

Arabidopsis Genome Initiative Code	emPAI Scores			Subcellular Localization		Predicted Domains or Protein Features
	Preparation 1	Preparation 2	Crude	X-GFP	GFP-X	
AT3G53320	0.28	8.48	0	MT	MT	No
AT5G57410	3.52	3.16	0	MT	MT	Afadin/α-actinin-binding domain
AT5G07590	2.89	1.59	0	Cytosol	Cytosol	WD40 (Trp-Asp REPEATING DOMAIN40) repeat
AT5G16730	0.35	2.60	0	MT	MT	Sepctrin/α-actinin domain and DUF827
AT1G15200	1.60	2.01	0	Cytosol	Cytosol	Pinin/Ser-Asp-Lys/memA domain
AT4G17620	1.91	0.43	0	Cytosol	Cytosol	Gly-rich protein
AT2G40070	1.32	0.40	0	MT	MT	Basic Pro-rich protein (BPP1)
AT5G24710	1.13	0.13	0	Cytosol	Cytosol	WD40 (Trp-Asp REPEATING DOMAIN40) repeat
AT3G13990	0.08	1.28	0	Cytosol	Cytosol	DUF1296 (kinase related)
AT2G07360	1.01	0.03	0	Cytosol	Cytosol	SH3 (SRC HOMOLOGY3) domain and Armadillo-type fold
AT1G14380	0.16	0.73	0	MT	MT	IQD28; IQ calmodulin-binding domain
AT1G19870	0.18	0.39	0	MT	MT	IQD32; IQ calmodulin-binding domain

which were eluted from the anion-exchange column, were analyzed by LC-MS/MS and queried against The Arabidopsis Information Resource release 10 protein data set. As a rough estimate of the relative protein abundance, we used the exponentially modified Protein Abundance Index (emPAI; Shinoda et al., 2010), which is based on the number of observed peptides divided by the number of theoretically observable peptides per protein. The highest emPAI scores of a given protein among all fractions of the two MAP-enriched preparations and the reference preparation were obtained, and the identified proteins are listed in decreasing order of their scores (Supplemental Tables S1–S4). For the list of MAP candidates, the emPAI scores of the reference preparation are also given (Supplemental Table S5).

The MAP-enriched preparations and the reference preparation (crude soluble proteins) showed highly different protein compositions. The majority of proteins identified in the MAP-enriched preparations had very low emPAI scores or were not identified in the reference preparation. Tubulins were well represented on this list, even though anion-exchange column-purified fractions containing large amounts of tubulins were excluded from the MS analysis. This MAP candidate list contained 36 previously reported MAPs and MT regulators, including MOR1 (Whittington et al., 2001), CLIP-ASSOCIATED PROTEIN (Ambrose et al., 2007), END BINDING1c (Komaki et al., 2010), MAP65 family proteins (Hussey et al., 2002), SPIRAL2 family proteins (Yao et al., 2008), MAP70 family proteins (Korolev et al., 2005), WAVE-DAMPENED2 family proteins (Perrin et al., 2007), MOVEMENT PROTEIN BINDING2C (Ruggenthaler et al., 2009), AUXIN-INDUCED IN ROOT CULTURES9 (Buschmann et al., 2006), RUNKEL (Krupnova et al., 2009), MAP190

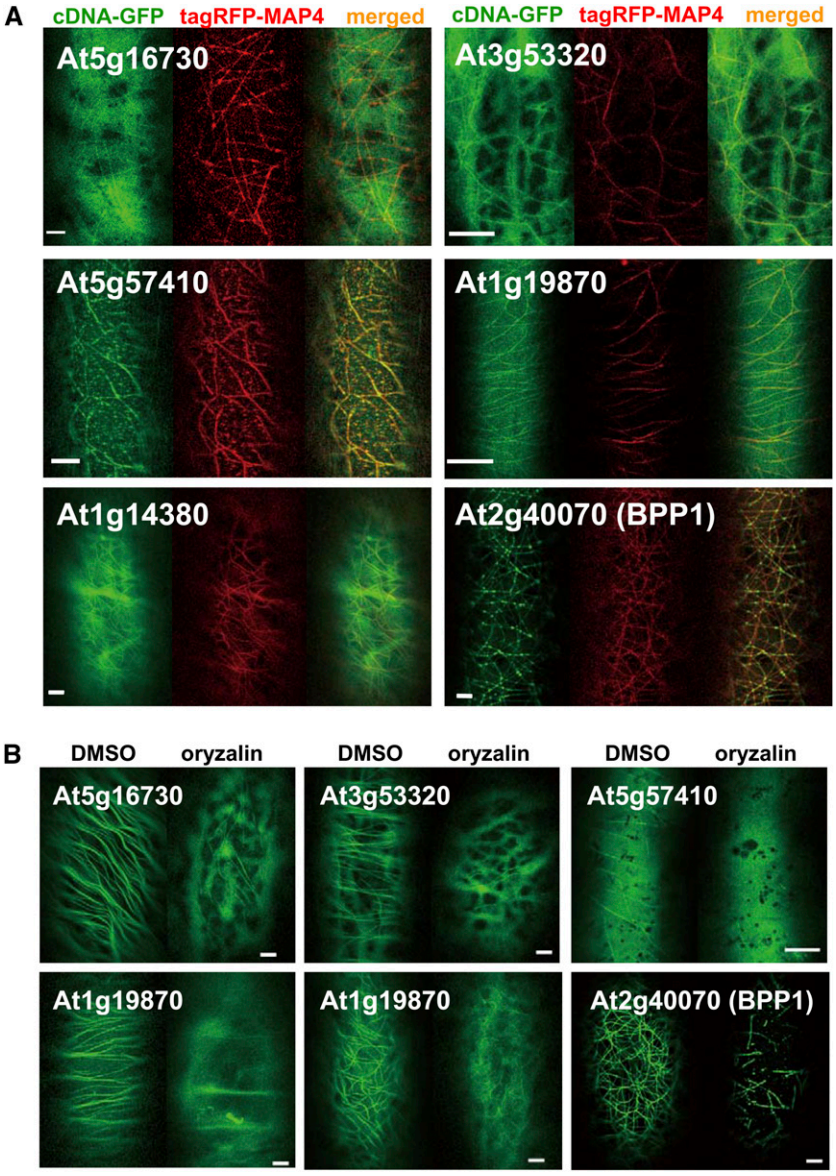

Figure 2. Localization of candidate MAPs on cortical MTs. Test proteins were fused to GFP at their C termini and transiently expressed in onion epidermal cells. A, An MT marker, tagRFP-MAP4, was coexpressed with the GFP fusions. B, Cells expressing GFP-fused proteins alone were treated for 30 min with either dimethyl sulfoxide (DMSO) or oryzalin (5 μM for all samples except BPP1-GFP-expressing cells, which received a dose of 10 μM). Bars = 10 μm. [See online article for color version of this figure.]

(Igarashi et al., 2000), MICROTUBULE DEPLETION DOMAIN1 (MIDD1; Oda et al., 2010), katanins (Sharp and Ross, 2012), and γ-tubulin ring complex proteins (Nakamura et al., 2010; Table I). These MAPs were absent or had very low emPAI scores in the crude preparation, indicating that they were significantly enriched by our MAP purification procedures. Some MT regulators, such as SPIRAL1 family proteins (Nakajima et al., 2006) and putative Arabidopsis MAPs, which had been shown to associate with MTs in in vivo or in vitro experiments (e.g. AUTOPHAGY-RELATED PROTEIN8; Ketelaar et al., 2004), were absent or were not identified with confidence in our MAP preparations (Supplemental Table S1). These proteins may have weak or negligible MT-binding activities under our MAP enrichment conditions. Alternatively, these proteins might have been absent in our crude cytoplasmic preparation from suspension-cultured cells. In the MAP preparations, we identified 23 proteins belonging to kinesin subfamilies 4, 5, 7, 13, and 14 and to the plant-specific kinesin subfamily (Zhu and Dixit, 2012; Table II). Kinesins belonging to subfamily 12 are proposed to recruit the Arabidopsis Fused kinase TWO-IN-ONE (TIO) to the phragmoplast midzone (Oh et al., 2012). Enrichment of TIO in MAP preparation 2, despite the absence of subfamily 12 kinesins (Supplemental Tables S1 and S2), implies that TIO might possess an intrinsic affinity for MTs.

To classify other identified proteins on a functional basis, we characterized the comprehensive data set according to the Gene Ontology annotations (ftp://ftp.arabidopsis.org/home/tair/Ontologies/Gene_Ontology/),

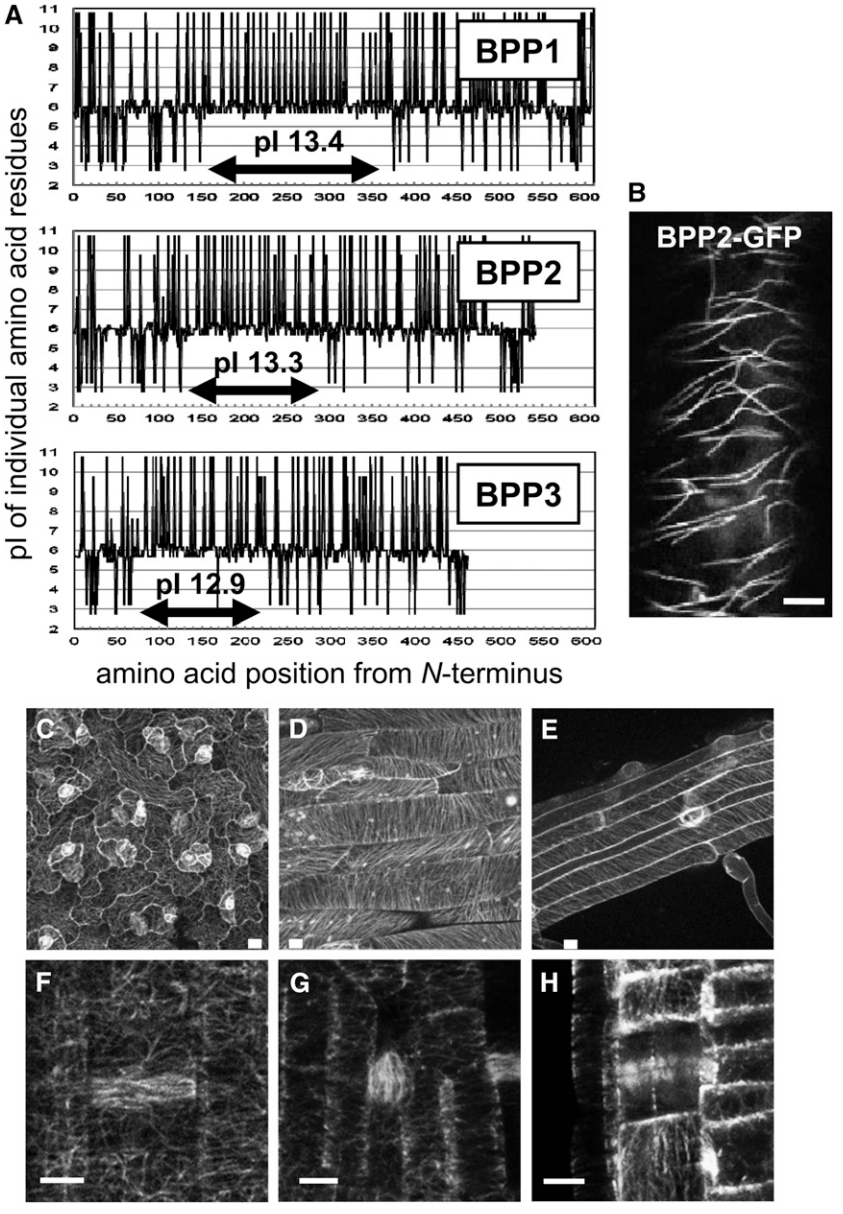

Figure 3. BPP1 is a MAP. A, Charge plots of the BPP family members. All BPPs contain highly basic regions devoid of acidic residues. B, Transiently expressed BPP2-GFP localizes to cortical MTs in onion epidermal cells (n = 4). C to H, Labeling of various MT arrays by BPP1-GFP. BPP1-GFP was expressed under its own regulatory elements in 11-d-old transgenic Arabidopsis plants. C, Leaf pavement cells. D, Hypocotyl epidermal cells. E, Root epidermal cells at the differentiation zone. F to H, Root epidermal cells. The preprophase band (F), mitotic spindle (G), and phragmoplast (H) were decorated by BPP1-GFP. Bars = 10 μm (B–E) and 5 μm (F–H).

followed by additional manual data mining of recently published work (Fig. 1D). Proteins with emPAI scores higher than 0.3 in either MAP preparation 1 or 2 (a total of 298 proteins) were subjected to the following analysis. Tubulins, MAPs, MT regulators, and kinesins constituted 20.5% (61 proteins) of the whole proteins. In the MAP-enriched proteome database, 23.5% (70 proteins) were annotated as being involved in RNA transcription, splicing, and metabolism; 5.0% (15 proteins) as having roles in DNA replication, repair, and structure; 7.7% (23 proteins) as being associated with the nucleolus, which includes RNA-processing functions; and 5.7% (17 proteins) as being involved in translation. Proteins belonging to these functional categories have been identified in animal MAP preparations (Liska et al., 2004; Patel et al., 2009; Gache et al., 2010) and in Arabidopsis tubulin-binding protein and MAP preparations (Chuong et al., 2004; Korolev et al., 2005). Nucleus- and nucleolus-localized ribonucleoproteins have been reported to regulate the organization of mitotic spindles (Hamada et al., 2009, and refs. therein). The putative tobacco subunit of the transcription and mRNA export factor complex, THO2, whose Arabidopsis ortholog (At1g24706) was highly enriched in our MAP preparations (Supplemental Table S1), was shown to directly bind MTs in vitro and to decorate cortical MTs in tobacco BY-2 cells (Hamada et al., 2009). Eukaryotic elongation factors EF-1α and EF-4F exhibit the biochemical properties of MAPs (Bokros et al., 1995; Moore and Cyr, 2000) and are enriched in our MAP preparations. Recent studies suggest that a large fraction of mRNAs are localized to subcellular compartments in polarized, asymmetric cells by mechanisms that involve the transport of RNA granules by molecular motors along the MT and actin cytoskeletons and result in spatially and temporally regulated translation (Martin and Ephrussi, 2009). Transcripts associated with cell division, spindle formation, and chromosome function copurify with mitotic MTs in *Xenopus laevis* egg extracts, implicating these proteins in spindle-localized translation (Sharp et al., 2011). MTs might also localize and spatially regulate translation in plant cells; however, this possibility remains to be explored.

Dynamins are large GTPases belonging to a protein superfamily that, in Arabidopsis, includes two classical dynamins and five phragmoplastin-like proteins (Hong et al., 2003a). Dynamin was previously characterized as a GTPase that can associate with MTs in vitro (Shpetner and Vallee, 1989; Obar et al., 1990; Hamada et al., 2006), and an Arabidopsis phragmoplastin-like protein was associated with MTs when expressed in tobacco cells (Hong et al., 2003b). Indeed, our MAP preparation 1 contained seven Arabidopsis dynamins of the dynamin and phragmoplastin subclasses with high emPAI scores (Supplemental Table S1). These Arabidopsis dynamins appear to function in cell plate formation during cytokinesis, but their interactions with phragmoplast MTs remain to be fully characterized (Konopka et al., 2006).

Furthermore, we identified proteins associated with organelles, endomembranes, and vesicle trafficking (Supplemental Table S1). Interestingly, 12 of the identified enzymes (4.0%) are involved in the metabolism of peroxisomes. Many of these peroxisomal proteins were recovered in MAP preparation 2, which presumably retained proteins with lower affinities for MTs than those purified in preparation 1. These peroxisomal proteins might possess MT-binding activities in addition to their well-characterized enzymatic activities, as demonstrated for the Arabidopsis peroxisomal multifunctional protein (Chuong et al., 2005). Alternatively, the outer membrane of peroxisomes might bind to MTs, resulting in partial cosedimentation of some peroxisomes with MTs during purification. Although actin filaments support the long-distance transport of peroxisomes in plant cells, these motile organelles were

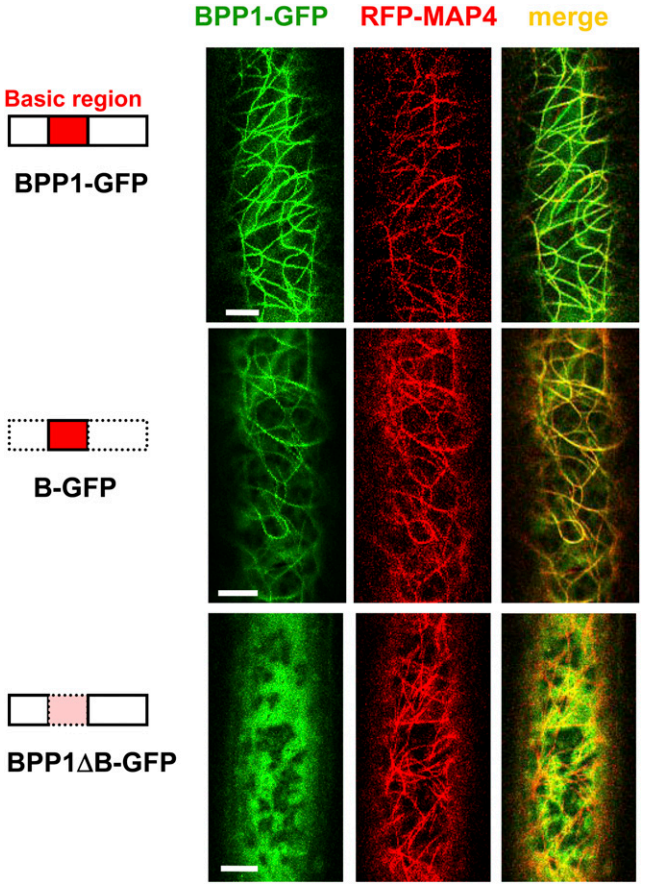

Figure 4. The basic region of BPP1 binds to MTs in vivo. Full-length BPP1 (top), the basic region of BPP1 (B; middle), and a BPP1 fragment lacking the basic region (BPP1ΔB; bottom) were fused to GFP and individually expressed in onion epidermal cells, together with tagRFP-MAP4. Full-length BPP1-GFP (n = 20) and B-GFP (n = 24) showed robust localization to cortical MTs in all transformed cells. In BPP1ΔB (n = 20), the majority of the transformed cells exhibited the diffuse labeling pattern typically shown in this figure, but three showed dotted fluorescent spots on filamentous structures (Supplemental Fig. S3). Bars = 10 μm. [See online article for color version of this figure.]

frequently observed to pause at cortical MTs (Chuong et al., 2005; Hamada et al., 2012). In humans, the evolutionarily conserved PEROXIN14 is not only a central component of the peroxisomal protein translocation machinery but is also required for peroxisome motility, serving as a membrane anchor for MTs (Bharti et al., 2011).

Identification of Novel Arabidopsis MAPs

The MAP-enriched preparations contained several dozen proteins (56 proteins with emPAI scores higher than 0.3) with functions that had not been characterized and could not be deduced from their primary structures (Supplemental Table S5). We selected 12 such proteins that appeared to be highly enriched in the MAP preparations and transiently expressed them as N- or C-terminal fusions to GFP by particle bombardment in the pavement cells of Arabidopsis leaves (Table III; Supplemental Fig. S1). Of the 12 MAP candidates, six labeled cortical filamentous structures, which appeared to be cortical MT arrays (Fig. 2). The At5g16730-encoded protein contained a spectrin/α-actinin domain (IPR018159) and a DUF827 domain of unknown functions, whereas the proteins encoded by At1g14380 and At1g19870 are, respectively, annotated as IQD28 and IQD32, which contain IQ calmodulin-binding regions (Abel et al., 2005). Interestingly, two other IQD proteins, IQD29 (At2g02790) and IQD31 (At1g74690), are also highly enriched in our MAP preparations (Supplemental Table S1), and these four IQD proteins form a distinct subgroup among the 33 IQD proteins in Arabidopsis (Abel et al., 2005). The protein encoded by At5g57410 has an Afadin/α-actinin-binding domain with a coiled-coil structure (IPR021622), which is found, for example, in Msd1 (for mitotic-spindle disanchored) of fission yeast (*Schizosaccharomyces pombe*), where it is required for anchoring the minus end of spindle MTs to the spindle pole body (Toya et al., 2007). The At2g40070 gene encodes a basic Pro-rich protein (BPP1) but has no known domains. The protein encoded by At3g53320 possesses no particular features in terms of amino acid composition or familiar domains. The patterns of the GFP-labeled filaments varied somewhat, possibly reflecting varying expression levels of the GFP fusions, ranging from dotted particles along the filaments (At5g57410) to bright, probably bundled, filaments (At5g16730 and BPP1). The remaining six proteins tested were broadly cytoplasmic or localized in patterns that did not resemble MTs (data not shown).

We further characterized the cellular localization of these six putative MT-binding proteins by transiently expressing the GFP fusions of these proteins in onion (*Allium cepa*) epidermal cells, together with the red fluorescent MT marker tagRFP-MAP4 (Fig. 2A). Merged images of the GFP and red fluorescent protein signals indicated that these six proteins localized to cortical MTs. When the bombarded onion cells were treated with 5 μM oryzalin, an MT-depolymerizing drug, for 30 min, the cortical MTs were no longer labeled with the GFP fusions of these proteins (Fig. 2B). In the case of BPP1-GFP, efficient depolymerization of MTs required higher concentrations (e.g. 10 μM) of oryzalin, and even under such harsh drug treatment, some MT remnants persisted, indicating that transient overexpression of BPP1-GFP stabilizes MTs.

Taken together, these results demonstrate that the six Arabidopsis proteins enriched in the MAP preparations are previously uncharacterized MAPs.

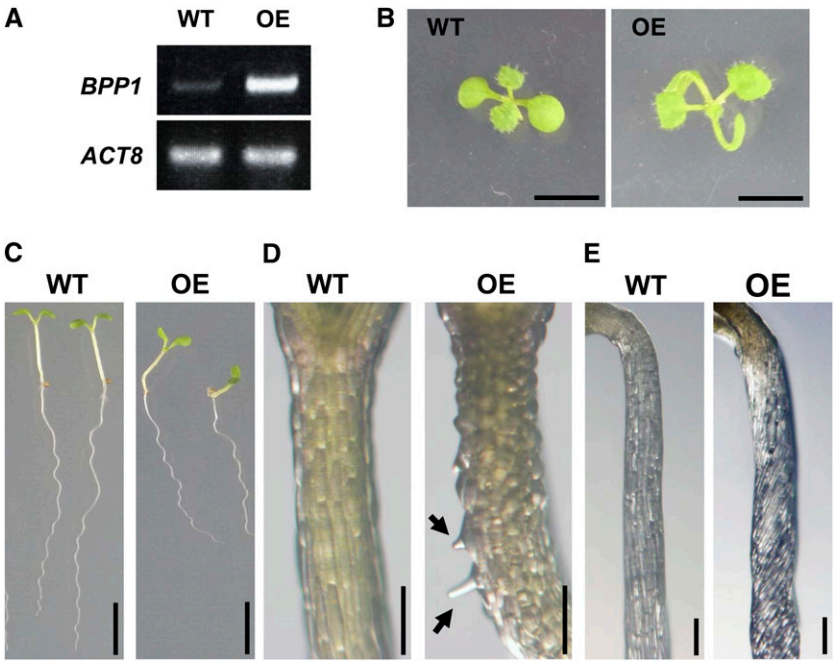

Figure 5. Overexpression of BPP1-GFP in Arabidopsis plants causes helical growth and abnormal cell expansion. A, RT-PCR analysis of BPP1 expression in wild-type (WT) and BPP1-GFP-overexpressing (OE) seedlings. *ACTIN8* (*ACT8*) was used as a control. B, Ten-day-old light-grown seedlings. C, Six-day-old seedlings grown in light on a vertically placed hard agar plate. D, Hypocotyls of 6-d-old light-grown seedlings. The epidermal cells of OE hypocotyls often produce ectopic protrusions (arrows). E, Etiolated hypocotyls of 5-d-old seedlings. Bars = 5 mm (B and C) and 200 μm (D and E). [See online article for color version of this figure.]

Characterization of BPP Family MAPs

BPP1, a 64-kD protein rich in Pro (11.2%) and basic amino acids (15.0%), belongs to a protein family that has seven members in Arabidopsis (Supplemental Fig. S2). BPP1, BPP2 (At3g09000), and BPP3 (At5g01280) form a subclade that, in addition to the basic region, contains three conserved motifs (Supplemental Fig. S2). The basic regions of BPPs contain no or few acidic amino acids and have average pI values higher than 12.9. A related Arabidopsis protein in the BPP1 clade (At2g38160; designated as BPP4) is truncated at the C-terminal region, is less basic than the other BPP members, and lacks one of the three motifs (Supplemental Fig. S2). Although BPP2 and BPP3 were not identified with confidence in the MAP preparations, peptide fragments of BPP2 are present in the MAP preparations (emPAI score of 0.07 in preparation 1; Supplemental Table S1). Indeed, when BPP2-GFP was transiently expressed in onion epidermal cells, the fusion protein labeled cortical MT-like structures (Fig. 3B). When the internal basic region of BPP1 was deleted and expressed transiently as a GFP fusion in onion epidermal cells together with tagRFP-MAP4, the truncated protein was mostly localized to the cytoplasm (Fig. 4; Supplemental Fig. S3). In contrast, the isolated basic region fused to GFP showed robust localization on cortical MTs. Thus, the highly basic regions of BPPs are mainly responsible for MT-binding activity. In vitro MT-binding assays will demonstrate whether BPP1 family proteins directly bind MTs.

Next, we stably expressed BPP1-GFP under the control of BPP1 regulatory elements in Arabidopsis plants (Fig. 3C). Cortical MT arrays were decorated with BPP1-GFP in the epidermal cells of leaves, hypocotyls, and roots. Mitotic MT structures, such as preprophase bands, spindle MTs, and phragmoplasts, were also labeled. Expression of the GUS reporter driven by the *BPP1* promoter indicated that *BPP1* is expressed at basal levels in many cell types, with stronger expression in meristematic regions and vasculature, and during early trichome development (Supplemental Fig. S4).

Three transfer DNA insertion mutants of *BPP1* yielded little or no *BPP1* transcript (Supplemental Fig. S5). These *bpp1* mutant alleles were indistinguishable from the wild type in terms of growth, development, and morphology, possibly because of the functional redundancy of *BPP1* with *BPP2* and *BPP3*. When BPP1 or BPP1-GFP was constitutively overexpressed under the control of the cauliflower mosaic virus 35S promoter, the transgenic Arabidopsis seedlings displayed slight right-handed helical twisting of the epidermal cell files in etiolated hypocotyls and petioles, resulting in an anticlockwise arrangement of cotyledons and young leaves (Fig. 5). When grown on hard agar plates that were placed vertically, primary roots of the BPP1-GFP-overexpressing seedlings grew toward the right side of the plates as viewed from the front. Epidermal cells in the apical region of light-grown hypocotyls often produced ectopic outgrowths that formed cone-like protrusions. Cortical MT arrays in leaf pavements cells that overexpressed BPP1-GFP were considerably ordered and aligned, largely transverse to the long axis of the cells (Fig. 6A). In the upper region of the light-grown hypocotyls of these plants, epidermal cells exhibited highly ordered MT arrays that were remarkably transverse to the cell's long axis (Fig. 6B). Epidermal protrusions (arrowheads) were surrounded by concentric cortical MT arrays. Quantification of MT distribution patterns in this cell type showed that GFP-β-TUBULIN6 (GFP-TUB6)-labeled MTs were widely distributed and did not align in particular patterns, as reported previously (Vineyard et al., 2013), whereas BPP1-GFP-labeled MTs in two independent lines

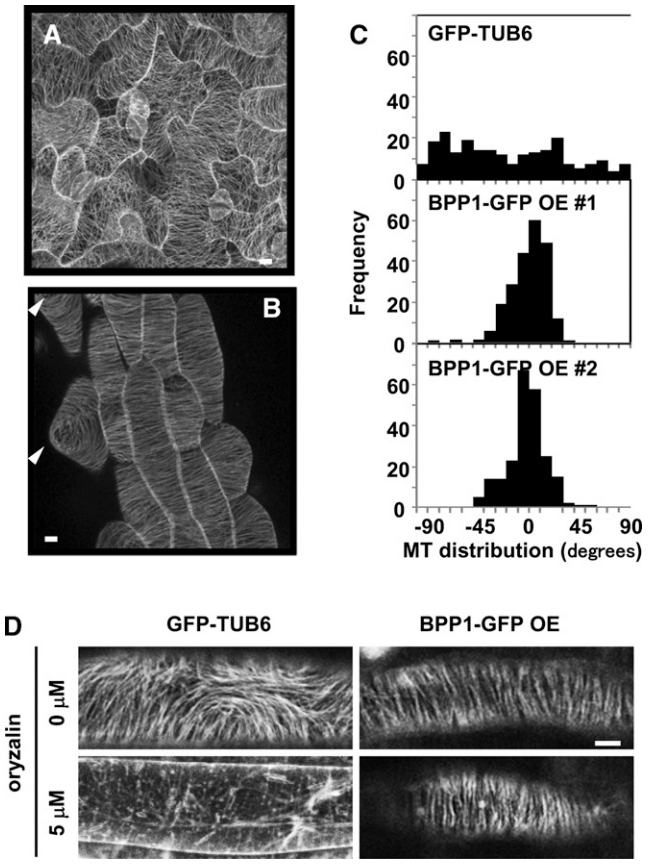

Figure 6. Overexpression of BPP1-GFP in Arabidopsis plants promotes the alignment of cortical MT arrays and increases MT stability. A, Leaf pavement cells. B, Epidermal cells of light-grown hypocotyls. Local protrusions are indicated by arrowheads. C, Distribution of cortical MTs in the epidermal cells of light-grown hypocotyls of GFP-TUB6 lines and two independent BPP1-GFP-overexpression (OE) lines. The angle perpendicular to the long axis of a cell was set as 0°. In GFP-TUB6, there was no MT distribution peak, whereas the average MT angles (±SD) were 4.1 ± 18.0 in BPP-GFP OE #1 and 9.1 ± 14.6 in BPP-GFP OE #2. A total of 225 MTs were analyzed in 15 cells for each line. D, Effects of oryzalin on cortical MTs. Arabidopsis seedlings (GFP-TUB6 and BPP1-GFP OE) were treated with dimethyl sulfoxide or 5 μM oryzalin for 30 min, and cortical MTs in hypocotyl epidermal cells were analyzed. Bar = 10 μm.

were aligned close to the transverse orientation (Fig. 6C). To examine MT stability, we treated the transgenic Arabidopsis seedlings with 5 μM of an MT-depolymerizing agent, oryzalin, for 30 min (Fig. 6D). Cortical MTs in the epidermal cells of light-grown seedlings that expressed GFP-TUB6 were mostly depolymerized by the oryzalin treatment, whereas MTs labeled with BPP1-GFP were resistant to this treatment, indicating that overexpression of BPP1-GFP stabilizes MTs.

The right-handed helical growth and ectopic protrusions in hypocotyl epidermal cells have been observed in *spiral1* mutants, in which cortical MTs are proposed to be more stabilized than those of the wild type (Furutani et al., 2000). In Arabidopsis *NimA-related kinase6* mutants, cortical MTs are excessively stabilized, and local outgrowth occurs in epidermal cells of the hypocotyls and petioles (Motose et al., 2011). Right-handed organ twisting has also been observed in MT-stabilizing Arabidopsis tubulin mutants (Ishida et al., 2007b) and in transgenic Arabidopsis plants overexpressing MT-stabilizing MAPs (Abe and Hashimoto, 2005; Korolev et al., 2007). We suggest that abnormal cell expansion in BPP1-overexpressing transgenic Arabidopsis plants is due to the excessive stabilization of cortical MTs.

CONCLUSION

In this study, we identified 727 Arabidopsis proteins that copurified with MT polymers. The majority of these proteins, which included many known MAPs, MT regulators, and kinesins, likely have considerable affinities toward MTs, may be part of the protein complexes in which one or more subunits bind MTs directly, or may be associated with organelles or cellular components that copurify with MTs. Our MAP-enriched proteomics database included several dozen previously uncharacterized proteins. As our initial characterization of 12 representative MAP candidates from the list revealed that six are bona fide MAPs, this database likely contains numerous hitherto unknown plant MAPs. Plant proteins that have been characterized as having functions and phenotypes not related to MTs may also be used to query this MAP-enriched proteomics database to search for possible interactions with MTs. A high-quality and comprehensive MAP database will greatly assist functional plant biology studies that focus on the MT cytoskeleton.

MATERIALS AND METHODS

Plant Materials and Growth Conditions

Cell suspension cultures of the Arabidopsis (*Arabidopsis thaliana*) cell line MM2d were grown in darkness in modified Linsmaier and Skoog medium on a gyratory shaker at 130 rpm and a constant temperature of 27°C as described (Menges and Murray, 2002; Hamada et al., 2006). The cultures were maintained by weekly dilution; 3 mL of 7-d-old MM2d cells was transferred to 95 mL of fresh medium in 300-mL flasks. Arabidopsis plants (Columbia [Col-0] ecotype) were grown as described (Nakamura et al., 2012). The GFP-TUB6 MT marker line has been reported (Nakamura et al., 2004).

Preparation of MAP Fractions

Five-day-old MM2d suspension cells were collected and converted to protoplasts by incubation in 2% (w/v) Sumizyme C and 0.2% (w/v) Sumizyme AP2 (Shin-Nihon Chemical) in 0.45 M sorbitol (pH 5.5) at 30°C for 2 h. Vacuoles were removed from protoplasts by density gradient centrifugation in a Percoll solution containing 27% (v/v) Percoll (GE Healthcare), 6.5 mM HEPES-KOH (pH 7.3), 0.49 M Suc, and 0.63 M sorbitol at 25,000*g* for 30 min. Evacuolated miniprotoplasts were collected, suspended in 1.5 volumes of ice-cold extraction buffer containing 50 mM PIPES-KOH (pH 7.0), 10 mM EGTA, 10% (w/v) Suc, 2 mM $MgCl_2$, 1% (w/v) casein, 1× protease inhibitor cocktail complete (Roche), 1 mM phenylmethylsulfonyl fluoride, and 4 mM dithiothreitol (DTT) and then homogenized with a Teflon homogenizer. After the homogenate was centrifuged at 170,000*g* at 2°C for 30 min, the supernatant was supplemented with 1 mM GTP and taxol (Paclitaxel; LC Laboratories) to a final concentration of 20 μM and incubated at 30°C for 8 min to polymerize the endogenous tubulin. MTs were collected by centrifugation at 23,000*g* for 10 min, were suspended in cold depolymerization buffer containing 20 mM PIPES-KOH (pH 7.0), 0.4 M NaCl (or 0.15 M NaCl, where specified), 1 mM $MgCl_2$, 1 mM $CaCl_2$, 1/10× protease inhibitor cocktail complete (Roche), 1 mM phenylmethylsulfonyl fluoride, and 1 mM DTT, and were kept on ice for 20 min. MAPs and tubulin were recovered in the supernatant after centrifugation at 250,000*g* for 5 min at 2°C, diluted with four volumes of the extraction buffer, and further purified by a second cycle of MT polymerization/depolymerization using the procedure described above. The purified MAP fractions and the crude cell extracts were applied to an anion-exchange column (Hi-trap Q; GE Healthcare) and eluted with a linear NaCl gradient from 0 to 1 M.

To evaluate protein profiles, aliquots of the eluted protein fractions were separated by SDS-PAGE on 7.5% acrylamide gels and stained with Coomassie Brilliant Blue.

Mass Spectrometry

Protein fractions, eluted from the anion-exchange column, were dialyzed, either individually or combined, against a buffer containing 20 mM ammonium bicarbonate and 5 mM DTT at 4°C. To exclude excess tubulin peptides, the eluted fractions containing large amounts of tubulin (fractions 18–28 in preparation 1 and fractions 15–23 in preparation 2) were not analyzed. Peptide preparation and LC-MS/MS analyses were performed as described previously (Fujiwara et al., 2009). Dialyzed samples were incubated for 1 h at 37°C and subsequently incubated with 25 mM iodoacetamide for 1 h at 37°C in the dark for alkylation. To stop the reaction, 14.2 mM DTT was added to the samples. The samples were digested overnight in 0.1 μg μL^{-1} trypsin at 37°C and then analyzed using the LTQ-Orbitrap XL-HTC-PAL system (Fujiwara et al., 2009). MS/MS spectra were matched against the Arabidopsis proteome (The Arabidopsis Information Resource release 10) using the MASCOT server (version 2.4).

Transient Expression in Onion and Arabidopsis Cells

Plasmids harboring a candidate MAP (2 μg) and the tagRFP-MAP4 MT marker plasmid (2 μg) were mixed with 1.5 mg of 1.6-μm gold particles suspended in 19.2% glycerol, 962 mM $CaCl_2$, and 1.5% spermidine for 30 min at room temperature, washed sequentially with 70% ethanol and 100% ethanol, and then cobombarded into leaf epidermis cells of 16- to 20-d-old Arabidopsis plants or onion (*Allium cepa*) epidermal peels using the PDS-1000/He Biolistic Particle Delivery System (Bio-Rad) equipped with 1,100-p.s.i. rupture disks. After incubation for 14 h in a moist petri dish in the dark, transfected cells were observed with a Nikon D-ECLIPSE C2 confocal microscope as a stack of confocal sections at 1-μm intervals through the cell cortex. GFP was excited at 488 nm and tagRFP at 543 nm using an ET514/30 and ET585/65 band-pass emission filter, respectively. Images were processed using Image J (National Institutes of Health) and Photoshop Elements 8 (Adobe Systems).

Candidate MAP complementary DNAs (cDNAs) were amplified by reverse transcription (RT)-PCR using total RNA from Arabidopsis Col-0 seedlings and the BP reaction and cloned into pDONRzeo. The cloned cDNA fragments were then transferred by the LB reaction to Gateway binary vector pGWB5 to generate 35S::GFP-MAP constructs and to vector pGWB6 to generate 35S::MAP-GFP constructs (Nakagawa et al., 2007). A MAP4 MT-binding domain was amplified by PCR from a GFP-MAP4 vector (a kind gift from Martin Hülskamp) and inserted after the tagRFP sequence in pHSG399 (Takara Bio). The tagRFP-MAP4 fragment was then inserted between the 35S

promoter and the NOS terminator of a pUC19 derivative, into which two extra restriction sites (*Asc*I and *Not*I) were added at the multiple cloning site.

A BPP1ΔB construct, in which the conserved basic region (amino acids 152–372) was deleted, was constructed by inverse PCR of the BPP1/pDONRzeo construct using two primers, 5′-TGCAGCAGACTCTGTTGAGG-3′ and 5′-CCGTCAGACATGCCTGGTTTC-3′. A construct that expressed only the basic region was generated from the BPP1/pDONRzeo construct by two rounds of inverse PCR using first-round primers 5′-CTTCCATGGTCTT-GACCTCAC-3′ and 5′-TACCCAGCTTTCTTGTACAAAG-3′ and second-round primers 5′-CATTAAGCCTGCTTTTTTGTAC-3′ and 5′-AGGAACCATCTAA-CATCTAGAC-3′.

Transgenic Plants

Agrobacterium tumefaciens strain GV3101 (pMP90) harboring binary vectors was used to transform Arabidopsis plants by the floral dip method (Clough and Bent, 1998).

A BPP1 genomic fragment, including the region 2,557 bp upstream of the start codon and 969-bp downstream of the stop codon, was cloned into pDONRzeo by PCR and the BP reaction. Juxtaposed *Sal*I and *Not*I tandem sites were introduced before the stop codon of the genomic BPP1 fragment by PCR. A PCR-amplified GFP fragment (without a stop codon) containing *Sal*I and *Not*I sites at its ends was inserted into the engineered genomic BPP1 clone, and the resulting BPP1-GFP genomic fragment was transferred to Gateway binary vector pGWB1 (Nakagawa et al., 2007) by the LB reaction. The 2,557-bp 5′ upstream fragment was transferred to Gateway binary vector pGWB3 (Nakagawa et al., 2007) by the LB reaction to generate a BPP1 promoter::GUS construct.

BPP1 and BPP2 cDNAs were amplified by RT-PCR using total RNA from Arabidopsis Col-0 seedlings and the BP reaction and cloned into pDONRzeo. The cloned cDNA fragments were then transferred by the LB reaction to Gateway binary vector pGWB2 to generate a 35S::BPP1 construct and to vector pGWB6 to generate a 35S::BPP1-GFP construct and a 35S::BPP2-GFP construct (Nakagawa et al., 2007).

MTs were analyzed with a Nikon C2 confocal microscope, as described above, as a stack of images at 1-μm intervals through the *z* axis.

RT-PCR Analysis

Total RNA was extracted using an RNeasy Plant Mini kit (Qiagen), and first-strand cDNA was synthesized with SuperScript II reverse transcriptase (Life Technologies). *BPP1* was amplified by PCR using the primer pairs 5′-GTACGCCTCTATTTCCATCG-3′ and 5′-GTTGATGATCTTCCAGT-GGG-3′ for the analysis of *bpp1* mutants and BPP1-GFP overexpression lines and 5′-CTCTGTTCCTGCGGTTAATC-3′ and 5′-TCTCCCTTGTAAGCTTGCAG-3′ for the analysis of *bpp1* mutants. ACT8 cDNA was amplified using the primers 5′-GCAGCATGAAGATTAAGGTCG-3′ and 5′-GAAAGAAATGTGATCCCGTC-3′. PCR was performed under the standard conditions of 20 cycles for the analysis of BPP1-GFP overexpression lines and 23 cycles for the analysis of *bpp1* mutants.

Sequence data from this article can be found in the GenBank/EMBL data libraries under accession numbers At2g40070 (*BPP1*), At3g09000 (*BPP2*), At5g01280 (*BPP3*), At2g38160 (*BPP4*), At1g27850 (*BPP5*), At3g0867 (*BPP6*), and At3g51540 (*BPP7*).

Supplemental Data

The following materials are available in the online version of this article.

Supplemental Figure S1. Subcellular localization of candidate MAPs in Arabidopsis cells.

Supplemental Figure S2. BPP family proteins.

Supplemental Figure S3. Minor localization pattern of BPP1Δ-GFP in onion cells.

Supplemental Figure S4. GUS staining patterns of the 2.6-kb BPP1 promoter in Arabidopsis seedlings.

Supplemental Figure S5. Transfer DNA insertion alleles of *bpp1* mutants.

Supplemental Table S1. Summary of MAP and crude preparations.

Supplemental Table S2. MAP preparation 1.

Supplemental Table S3. MAP preparation 2.

Supplemental Table S4. Crude reference preparation.

Supplemental Table S5. Novel MAP candidates.

ACKNOWLEDGMENTS

We thank Martin Hülskamp (Universität Tübingen) for the GFP-MAP4 vector and Tsuyoshi Nakagawa (Shimane University) for the pGWB vectors. The SALK Institute Genomic Analysis Laboratory, the Institut National de la Recherche Agronomique, and the Arabidopsis Biological Resource Center are acknowledged for providing the transfer DNA knockout alleles and the genomic DNA and cDNA clones.

Received July 25, 2013; accepted October 15, 2013; published October 17, 2013.

LITERATURE CITED

Abe T, Hashimoto T (2005) Altered microtubule dynamics by expression of modified alpha-tubulin protein causes right-handed helical growth in transgenic Arabidopsis plants. Plant J **43:** 191–204

Abel S, Savchenko T, Levy M (2005) Genome-wide comparative analysis of the IQD gene families in Arabidopsis thaliana and Oryza sativa. BMC Evol Biol **5:** 72

Ambrose JC, Shoji T, Kotzer AM, Pighin JA, Wasteneys GO (2007) The *Arabidopsis* CLASP gene encodes a microtubule-associated protein involved in cell expansion and division. Plant Cell **19:** 2763–2775

Bharti P, Schliebs W, Schievelbusch T, Neuhaus A, David C, Kock K, Herrmann C, Meyer HE, Wiese S, Warscheid B, et al (2011) PEX14 is required for microtubule-based peroxisome motility in human cells. J Cell Sci **124:** 1759–1768

Bokros CL, Hugdahl JD, Kim HH, Hanesworth VR, van Heerden A, Browning KS, Morejohn LC (1995) Function of the p86 subunit of eukaryotic initiation factor (iso)4F as a microtubule-associated protein in plant cells. Proc Natl Acad Sci USA **92:** 7120–7124

Buschmann H, Chan J, Sanchez-Pulido L, Andrade-Navarro MA, Doonan JH, Lloyd CW (2006) Microtubule-associated AIR9 recognizes the cortical division site at preprophase and cell-plate insertion. Curr Biol **16:** 1938–1943

Chang-Jie J, Sonobe S (1993) Identification and preliminary characterization of a 65 kDa higher-plant microtubule-associated protein. J Cell Sci **105:** 891–901

Chuong SD, Good AG, Taylor GJ, Freeman MC, Moorhead GB, Muench DG (2004) Large-scale identification of tubulin-binding proteins provides insight on subcellular trafficking, metabolic channeling, and signaling in plant cells. Mol Cell Proteomics **3:** 970–983

Chuong SD, Park NI, Freeman MC, Mullen RT, Muench DG (2005) The peroxisomal multifunctional protein interacts with cortical microtubules in plant cells. BMC Cell Biol **6:** 40

Clough SJ, Bent AF (1998) Floral dip: a simplified method for Agrobacterium-mediated transformation of Arabidopsis thaliana. Plant J **16:** 735–743

Desai A, Mitchison TJ (1997) Microtubule polymerization dynamics. Annu Rev Cell Dev Biol **13:** 83–117

Fujiwara M, Hamada S, Hiratsuka M, Fukao Y, Kawasaki T, Shimamoto K (2009) Proteome analysis of detergent-resistant membranes (DRMs) associated with OsRac1-mediated innate immunity in rice. Plant Cell Physiol **50:** 1191–1200

Furutani I, Watanabe Y, Prieto R, Masukawa M, Suzuki K, Naoi K, Thitamadee S, Shikanai T, Hashimoto T (2000) The SPIRAL genes are required for directional control of cell elongation in Arabidopsis thaliana. Development **127:** 4443–4453

Gache V, Waridel P, Winter C, Juhem A, Schroeder M, Shevchenko A, Popov AV (2010) Xenopus meiotic microtubule-associated interactome. PLoS ONE **5:** e9248

Gardiner J, Marc J (2003) Putative microtubule-associated proteins from the Arabidopsis genome. Protoplasma **222:** 61–74

Hamada T (2007) Microtubule-associated proteins in higher plants. J Plant Res **120:** 79–98

Hamada T, Igarashi H, Itoh TJ, Shimmen T, Sonobe S (2004) Characterization of a 200 kDa microtubule-associated protein of tobacco BY-2

cells, a member of the XMAP215/MOR1 family. Plant Cell Physiol **45:** 1233–1242

Hamada T, Igarashi H, Taguchi R, Fujiwara M, Fukao Y, Shimmen T, Yokota E, Sonobe S (2009) The putative RNA-processing protein, THO2, is a microtubule-associated protein in tobacco. Plant Cell Physiol **50:** 801–811

Hamada T, Igarashi H, Yao M, Hashimoto T, Shimmen T, Sonobe S (2006) Purification and characterization of plant dynamin from tobacco BY-2 cells. Plant Cell Physiol **47:** 1175–1181

Hamada T, Tominaga M, Fukaya T, Nakamura M, Nakano A, Watanabe Y, Hashimoto T, Baskin TI (2012) RNA processing bodies, peroxisomes, Golgi bodies, mitochondria, and endoplasmic reticulum tubule junctions frequently pause at cortical microtubules. Plant Cell Physiol **53:** 699–708

Hong Z, Bednarek SY, Blumwald E, Hwang I, Jurgens G, Menzel D, Osteryoung KW, Raikhel NV, Shinozaki K, Tsutsumi N, et al (2003a) A unified nomenclature for Arabidopsis dynamin-related large GTPases based on homology and possible functions. Plant Mol Biol **53:** 261–265

Hong Z, Geisler-Lee CJ, Zhang Z, Verma DP (2003b) Phragmoplastin dynamics: multiple forms, microtubule association and their roles in cell plate formation in plants. Plant Mol Biol **53:** 297–312

Hussey PJ, Hawkins TJ, Igarashi H, Kaloriti D, Smertenko A (2002) The plant cytoskeleton: recent advances in the study of the plant microtubule-associated proteins MAP-65, MAP-190 and the Xenopus MAP215-like protein, MOR1. Plant Mol Biol **50:** 915–924

Igarashi H, Orii H, Mori H, Shimmen T, Sonobe S (2000) Isolation of a novel 190 kDa protein from tobacco BY-2 cells: possible involvement in the interaction between actin filaments and microtubules. Plant Cell Physiol **41:** 920–931

Ishida T, Kaneko Y, Iwano M, Hashimoto T (2007a) Helical microtubule arrays in a collection of twisting tubulin mutants of Arabidopsis thaliana. Proc Natl Acad Sci USA **104:** 8544–8549

Ishida T, Thitamadee S, Hashimoto T (2007b) Twisted growth and organization of cortical microtubules. J Plant Res **120:** 61–70

Ketelaar T, Voss C, Dimmock SA, Thumm M, Hussey PJ (2004) Arabidopsis homologues of the autophagy protein Atg8 are a novel family of microtubule binding proteins. FEBS Lett **567:** 302–306

Komaki S, Abe T, Coutuer S, Inzé D, Russinova E, Hashimoto T (2010) Nuclear-localized subtype of end-binding 1 protein regulates spindle organization in Arabidopsis. J Cell Sci **123:** 451–459

Konopka CA, Schleede JB, Skop AR, Bednarek SY (2006) Dynamin and cytokinesis. Traffic **7:** 239–247

Korolev AV, Chan J, Naldrett MJ, Doonan JH, Lloyd CW (2005) Identification of a novel family of 70 kDa microtubule-associated proteins in Arabidopsis cells. Plant J **42:** 547–555

Korolev AV, Buschmann H, Doonan JH, Lloyd CW (2007) AtMAP70-5, a divergent member of the MAP70 family of microtubule-associated proteins, is required for anisotropic cell growth in Arabidopsis. J Cell Sci **120:** 2241–2247

Krupnova T, Sasabe M, Ghebreghiorghis L, Gruber CW, Hamada T, Dehmel V, Strompen G, Stierhof YD, Lukowitz W, Kemmerling B, et al (2009) Microtubule-associated kinase-like protein RUNKEL needed [corrected] for cell plate expansion in Arabidopsis cytokinesis. Curr Biol **19:** 518–523

Liska AJ, Popov AV, Sunyaev S, Coughlin P, Habermann B, Shevchenko A, Bork P, Karsenti E, Shevchenko A (2004) Homology-based functional proteomics by mass spectrometry: application to the Xenopus microtubule-associated proteome. Proteomics **4:** 2707–2721

Lloyd C, Hussey P (2001) Microtubule-associated proteins in plants: why we need a MAP. Nat Rev Mol Cell Biol **2:** 40–47

Maiato H, Sampaio P, Sunkel CE (2004) Microtubule-associated proteins and their essential roles during mitosis. Int Rev Cytol **241:** 53–153

Mandelkow E, Mandelkow EM (1995) Microtubules and microtubule-associated proteins. Curr Opin Cell Biol **7:** 72–81

Martin KC, Ephrussi A (2009) mRNA localization: gene expression in the spatial dimension. Cell **136:** 719–730

Menges M, Murray JA (2002) Synchronous Arabidopsis suspension cultures for analysis of cell-cycle gene activity. Plant J **30:** 203–212

Moore RC, Cyr RJ (2000) Association between elongation factor-1alpha and microtubules in vivo is domain dependent and conditional. Cell Motil Cytoskeleton **45:** 279–292

Motose H, Hamada T, Yoshimoto K, Murata T, Hasebe M, Watanabe Y, Hashimoto T, Sakai T, Takahashi T (2011) NIMA-related kinases 6, 4, and 5 interact with each other to regulate microtubule organization during epidermal cell expansion in Arabidopsis thaliana. Plant J **67:** 993–1005

Nakagawa T, Kurose T, Hino T, Tanaka K, Kawamukai M, Niwa Y, Toyooka K, Matsuoka K, Jinbo T, Kimura T (2007) Development of series of gateway binary vectors, pGWBs, for realizing efficient construction of fusion genes for plant transformation. J Biosci Bioeng **104:** 34–41

Nakajima K, Kawamura T, Hashimoto T (2006) Role of the SPIRAL1 gene family in anisotropic growth of Arabidopsis thaliana. Plant Cell Physiol **47:** 513–522

Nakamura M, Ehrhardt DW, Hashimoto T (2010) Microtubule and katanin-dependent dynamics of microtubule nucleation complexes in the acentrosomal Arabidopsis cortical array. Nat Cell Biol **12:** 1064–1070

Nakamura M, Naoi K, Shoji T, Hashimoto T (2004) Low concentrations of propyzamide and oryzalin alter microtubule dynamics in Arabidopsis epidermal cells. Plant Cell Physiol **45:** 1330–1334

Nakamura M, Yagi N, Kato T, Fujita S, Kawashima N, Ehrhardt DW, Hashimoto T (2012) Arabidopsis GCP3-interacting protein 1/MOZART 1 is an integral component of the γ-tubulin-containing microtubule nucleating complex. Plant J **71:** 216–225

Obar RA, Collins CA, Hammarback JA, Shpetner HS, Vallee RB (1990) Molecular cloning of the microtubule-associated mechanochemical enzyme dynamin reveals homology with a new family of GTP-binding proteins. Nature **347:** 256–261

Oda Y, Iida Y, Kondo Y, Fukuda H (2010) Wood cell-wall structure requires local 2D-microtubule disassembly by a novel plasma membrane-anchored protein. Curr Biol **20:** 1197–1202

Oh SA, Allen T, Kim GJ, Sidorova A, Borg M, Park SK, Twell D (2012) Arabidopsis Fused kinase and the Kinesin-12 subfamily constitute a signalling module required for phragmoplast expansion. Plant J **72:** 308–319

Patel PC, Fisher KH, Yang EC, Deane CM, Harrison RE (2009) Proteomic analysis of microtubule-associated proteins during macrophage activation. Mol Cell Proteomics **8:** 2500–2514

Perrin RM, Wang Y, Yuen CY, Will J, Masson PH (2007) WVD2 is a novel microtubule-associated protein in Arabidopsis thaliana. Plant J **49:** 961–971

Ruggenthaler P, Fichtenbauer D, Krasensky J, Jonak C, Waigmann E (2009) Microtubule-associated protein AtMPB2C plays a role in organization of cortical microtubules, stomata patterning, and tobamovirus infectivity. Plant Physiol **149:** 1354–1365

Sedbrook JC, Kaloriti D (2008) Microtubules, MAPs and plant directional cell expansion. Trends Plant Sci **13:** 303–310

Sharp DJ, Ross JL (2012) Microtubule-severing enzymes at the cutting edge. J Cell Sci **125:** 2561–2569

Sharp JA, Plant JJ, Ohsumi TK, Borowsky M, Blower MD (2011) Functional analysis of the microtubule-interacting transcriptome. Mol Biol Cell **22:** 4312–4323

Shinoda K, Tomita M, Ishihama Y (2010) emPAI Calc: for the estimation of protein abundance from large-scale identification data by liquid chromatography-tandem mass spectrometry. Bioinformatics **26:** 576–577

Shpetner HS, Vallee RB (1989) Identification of dynamin, a novel mechanochemical enzyme that mediates interactions between microtubules. Cell **59:** 421–432

Toya M, Sato M, Haselmann U, Asakawa K, Brunner D, Antony C, Toda T (2007) Gamma-tubulin complex-mediated anchoring of spindle microtubules to spindle-pole bodies requires Msd1 in fission yeast. Nat Cell Biol **9:** 646–653

Vineyard L, Elliott A, Dhingra S, Lucas JR, Shaw SL (2013) Progressive transverse microtubule array organization in hormone-induced *Arabidopsis* hypocotyl cells. Plant Cell **25:** 662–676

Whittington AT, Vugrek O, Wei KJ, Hasenbein NG, Sugimoto K, Rashbrooke MC, Wasteneys GO (2001) MOR1 is essential for organizing cortical microtubules in plants. Nature **411:** 610–613

Yao M, Wakamatsu Y, Itoh TJ, Shoji T, Hashimoto T (2008) Arabidopsis SPIRAL2 promotes uninterrupted microtubule growth by suppressing the pause state of microtubule dynamics. J Cell Sci **121:** 2372–2381

Zhu C, Dixit R (2012) Functions of the Arabidopsis kinesin superfamily of microtubule-based motor proteins. Protoplasma **249:** 887–899